DOE/PC/89754--T6

DOE/PC/89754--T6

DE92 018751

PROJECT STATUS REPORT

1992

Report Date: June 21, 1989

Report No : 1

Report Period: 2/27/89-5/31/89

CONTRACT TITLE: The Kinetics of Sulfation of Calcium Oxide

CONTRACT NUMBER: DE-FG-22-89PC89754

CONTRACTOR NAME: M.I.T., 66-466

Cambridge, MA 02139

PRINCIPAL INVESTIGATORS: A.F. Sarofim and J.P. Longwell

CONTRACT PERIOD: 27 February 1989 to 26 August 1990

DISCLAIMER

1. INTRODUCTION.

Sulfur emissions control is important for many fossil fuel applications, and mandatory to comply with environmental standards. Many techniques are available for the desulfurization of coal combustion processes. What is generally known as the LIMB process (Lime Injection Multistage Burner), however, carries great promises for an easy implementation and a low cost.

Temperatures found in coal-fired boilers are usually rather high (1500-2000^{o}C), but the residence time is less than 2 seconds. The temperature history the limestone is subject to will have a determining effect on its reactivity. This can be attributed to changes in physical structure (sintering). Several investigators (Borgwardt, 1987; Sarofim et al, 1987) showed that the composition of the origiral stone is also very important: hydrates react much faster than carbonates, and, to a lesser extent, the concentration of other oxides affected the reaction.

Studies of the sulfation rate behavior show an initial fast rate followed by a rate decrease. It is generally agreed that product layer diffusion limitations are the explanation for this behavior. Many investigators tried to model this observed rate change, more or less successfully. No agreement has been reached, however, as to the value of the product layer diffusivity.

Hence, in this work we want to investigate the mechanism of this process. In addition to understanding the initial kinetics, two questions will be focused on. First, we should understand

what is diffusing. It appears that the driving force for this diffusion phenomenon is not first order with the SO_2 concentration in the gas. This would indicate that some other, intermediary step is occurring. The second question concerns the composition of the product layer. Different conditions at the start of the reaction were observed to produce different diffusion rates at a later stage. The microscopic appearance of the product layer also appeared to be different.

2. CHOICE OF SAMPLE

In order to avoid pore diffusion limitations, and dependence of the result on the physical structure of the material, different types of sample were used in this study.

2.1. CaO Single Crystals

Calcium Oxide Single Crystals are composed of large nonporous rhomboedric grains, each being a monocrystal. This material cannot be found in nature, because it is very reactive with atmospheric moisture. It must therefore be grown and kept in an organic liquid, free from all water contamination. As a result, it is an expensive material, that must be used in a very careful way.

Its advantages, however, are important. Because of its macroscopic size (the smallest size it can be ground to is about 20 μm), the diffusion can be modeled as a one-dimensional process. In addition, its structure is readily recognizable on

SEM pictures, and therefore the formation of a product layer can be followed easily.

Hydration, however, is unavoidable, and one can not assume that the reaction occurs with a CaO monocrystal, except at larger conversions, when the initial, dehydrated layer has completely reacted. Even then, however, hydration can have an effect due to the large number of nucleation sites it leaves behind, thus affecting grain size and composition of the product layer. Great care was taken to keep the sample in a dry atmosphere, but several runs had to be discarded as a result of hydration.

2.2 Synthetic Lime

The citric acid technique, developed by Marcilly et al. (1972), produces a synthetic lime composed of very porous particles (porosity between 90 and 95%), featuring non-porous, spherical granules with average diameter of 0.3 μm, which translates into a surface area of about 5 m^2/g. This product can be regarded as composed of large particles, 100 μm in diameter, which, with the above porosity, exhibit an effectiveness factor of 0.97. It can also be viewed as small non-porous CaO grains whose properties are halfway between the two previously described samples. They are large enough to be observable in the SEM, and still small enough to provide a measurable reaction rate that can be modeled by spherical grains.

The synthetic lime was prepared using the method described by Marcilly et al (1970). Calcium nitrate is dissolved in as little water as possible, together with an equimolar amount of

citric acid. This solution is rapidly dehydrated at low temperature (70°C), in a vacuum of at least 29" Hg. The material rises and creates a glassy solid foam. It is then pyrolysed at 400°C, and calcined at 1000°C for 4 hours. This procedure yields a very lose structure, consisting of grains approximately half a micron in size. If it is desired to add other oxides to this lime, one dissolves the correct amount of a soluble salt of this oxide in the aqueous solution at the first stage of the preparation.

This product was found especially useful to measure the initial reaction rate: the effectiveness factor of 0.97 indicates negligible pore diffusion limitations, and the large surface area produces a reasonably fast rate. Disadvantages, however, are twofold. First, CaO is very sensitive to moisture, and similarly as the monocrystalline CaO, will hydrate after some time, thus altering its structure. Second, the spherical granules that compose this material are often interconnected, or at least touching. When the reaction proceeds, these granules grow and start overlapping each other. Hence, the simple grain model is no longer applicable, and for accurate measurements of high conversion diffusivities, another model must be used.

2.3 Iceland Spar

Iceland Spar is a limestone (i.e. CaCO3) that is found in nature in a very pure form. Large single crystals of this material can readily be obtained. This product must be calcined to obtain the reactive lime, yielding thus a porous CaO. The

porosity of this sample, as long as no shrinking occurs, is 46%, the ratio of the molar volumes of calcium oxide and calcium carbonate. The pore size and the surface area, however, depend on the CO_2 back pressure present during decomposition (Snow, 1985; Hajaligol, 1987). In this work, the decomposition was always performed in an inert atmosphere, yielding a surface area of about 30 m^2/g.

Using the above values for porosity and surface area to calculate the Thiele Modulus of calcined Iceland Spar grains , about 15 to 20 μm in size, one obtains $\Phi = 0.9$, or an effectiveness factor of $\eta = 0.7$. This means that pore diffusion limitations must be considered, and that, if the pores are small enough, pore plugging will occur. Once all the pores are plugged, a much lower sulfation rate is observed, due to the diffusion through the external sulfate crust. In other words, we observe here the same diffusion as if we had started with nonporous grains.

The great advantage of using this material is that it can be calcined in situ, and hence the CaO produced doesn't enter in contact with atmospheric moisture. It is important to keep in mind , however, that the starting material is a porous CaO (see Fig 1), and hence contains many nucleation sites for the $CaSO_4$ product layer. One can therefore expect a different product layer composition from what is observed with monocrystalline CaO.

3. EQUIPMENT

3.1 TGA

The thermogravimetric analyzer was used most regularly to follow the reaction kinetics. The thermal balance, manufactured by Cahn Instruments, is sketched in Figure 2. It is described in detail by J. Floess (PhD thesis, 1985). The balance itself is held under a constant He flow, to avoid contact of aggressive SO_2 gas with the delicate electronics. The optimal flow rate through the balance was found to be 200 standard cubic centimeters per minute. A higher rate would create large temperature gradients around the sample pan. A lower rate would yield mass transfer limitations (see also J. Floess). The gas used typically consists of 5% O_2, 3000 ppm SO_2 and a balance of helium. Helium was chosen rather than nitrogen because of the higher diffusivity it provides for SO_2 and O_2. Different kinds of problems were encountered with the operation of the TGA. In the initial stages of this research, sulfuric acid was found to condensate on the balance wire, increasing the weight. The gases were then chosen to flow downward, such that condensation at the outlet of the reactor wouldn't affect the reading.

Mass transfer limitation was also found to affect the measurements. In order to avoid this, sample sizes of 0.6 mg or less had to be used. In addition, better results were obtained when sprinkling the sample on top of a quartzwool bed, instead of depositing the reacting lime on a platinum or alumina pan.

3.2 Scanning Electron Microscope

A scanning Electron Microscope, manufactured by Cambridge Instruments and equipped with a numerical image analyzer was used on a regular basis to obtain qualitative data necessary for the development of a model. Particle shapes and sizes were measured at different conversion, after preparation in the TGA.

The principle of the Scanning Electron Microscope requires that high energy electrons be conducted away from the sample. A conductive sample is therefore preferred, or otherwise a thin conducting gold or palladium layer can be deposited on the surface. The calcium oxide and calcium sulfate material used, however, was so non-conductive that a double layer of carbon and Palladium had to be used. Palladium replaced the gold because the X-ray fluorescence peak of gold and sulfur overlap each other which made it difficult to obtain a good estimate of the relative amount of sulfur and calcium with the X-ray spectrometer.

The numerical image analyzer was found very useful to avoid blurring of the image due to the charging of the sample.

4. EXPERIMENTAL PROCEDURE

4.1 Continuous runs

Because of the very hygroscopic character of our reactant, CaO, we must be very careful and manipulate it as much as possible in a controlled atmosphere. The grinding, sieving and storing was all done in a dry box with nitrogen atmosphere.

When a run is started, the TGA is first zeroed with the empty sample pan containing a piece of quartzwool (used to enhance the external diffusion rate), in the presence of purge gas. The sample pan is then taken to the dry box where the lime is sprinkled on top. The transport from the dry box to the TGA requires approximately 20 seconds.This is the only time when the sample is in direct contact with the atmosphere. The weight is immediately recorded from the TGA signal. In case iceland spar is used, the dry box doesn't need to be used since the starting material is $CaCO_3$ which is not hygroscopic.

At this point, the furnace is turned on and the temperature increased linearly to the final temperature. If hydration has occurred, a weight loss is observed when the temperature reaches 350°C. This is how we can monitor whether our sample is still good, or whether it must be replaced. When iceland spar is used, a weight loss occurs at 650°C, which is the decomposition temperature of carbonate in an inert atmosphere.

This heating period is taken to be typically 20 minutes. Another 10 to 15 minutes are needed for steady state to be reached. Then, the helium purge gas is replaced by the reactant gases, and the weight increase of the sample is recorded at regular (5 seconds) intervals. As a result of the switch of gases, an equilibration time of approximately one minute must be allowed before the measured weight can be trusted. When the initial rate is very fast, this inhibits us to measure it accurately.

If only the initial rate is needed, the run is terminated

after 30 to 40 minutes. Often, however, we are interested in the behavior of the diffusivity with time (or conversion). In this case, we can let the experiment run overnight.

4.2 Combination runs

When the results of continuous runs are analyzed, a number of observations were made that could not be explained with the classical diffusion theory (see also section 5):

(1) The diffusivity decreases with time (Fig 3)

(2) The order for SO_2 concentration is 0.5 rather than 1.

(3) The activation energy is much lower (about 16 kcal/mol) than expected for solid state diffusion.

These observations led to the double focus of this work: what is the diffusing compound, and what is the composition of the product layer. The former question relates to the driving force (chemical potential gradient), and the latter will affect the value of the diffusivity. The rate measurement we obtain is proportional to the diffusion rate, which is the product of diffusivity and potential gradient

$$F = D * \nabla\mu$$

In order to investigate one issue at a time, an experiment was designed where a product layer was formed under controlled conditions (temperature and SO_2 partial pressure), after which the conditions were changed and the rate measured. Doing so, we could investigate the effect of SO_2 concentration and the temperature on a partly reacted sample whose product layer was known to have constant properties (and hence a constant

diffusivity.)

The procedure followed is illustrated in Figure 4. It shows both the weight and the temperature trace as a function of time. For the heating period, the same approach was used as for the continuous runs. After having sulfated the sample for a fixed period of time, varying from 2.5 to 40 minutes, purge gas is introduced again and the conditions changed. The sulfation is then resumed, and the initial rate (in moles reacted/s gCaO) is recorded.

5. RESULTS AND ANALYSIS

5.1. Continuous Runs

As a first measure of the reaction rate the slope of the conversion versus time curve was taken at the origin. Except for iceland spar, where pore diffusion limitations don't allow to measure this rate, the other sample used exhibit a rate that is approximately proportional to their surface area. The Arrhenius plot shown in Figure 5 illustrates this clearly. Three series experiments are presented here. Results obtained with the synthetic lime exhibit a relatively low activation energy of 16 kcal/mol. The rate, for this sample, can be approximated by the following analytical expression:

$$k = 18*10^{-3} \exp(-8040/T) \quad mol/s\ m^2$$

Some experiments reported on Figure 5 were performed with submicron CaO ash. This material is composed of extremely small (0.02μm) calcium oxide (or hydroxide!) grains, clustered

together on a quartzwool pad. The higher activation energy obtained with this sample is probably due to the inaccuracy of the higher temperature results: because of the fast rate, the response time of the instrument interferes with the measurement, yielding an overestimated rate. The lower temperature results give a line that is almost parallel with the synthetic lime runs. The rate difference in absolute value is probably due to the error in estimated surface area of the submicron ash.

The higher temperature runs shown in the same Figure were performed by M. Snow (1985) in a drop tube furnace. The rate was calculated from the conversion measured after 1.8 seconds. These measurements were done with Iceland Spar, which exhibits an initial fast rate followed by pore plugging. As a result, it is expected that, since at high temperature the knee will occur much sooner, after 1.8 seconds the linear region is passed and the solid state diffusion region is reached. Therefore, the rate measured is slower than the actual rate, and the more so the higher the temperature. Hence a lower activation energy.

5.2. Diffusivity

5.2.1. Results

Using a simple grain model, it is possible to calculate the diffusivity of the reactant through the product layer at different moments during the reaction. For the synthetic lime, a grain model was used, with grain diameter derived from the surface area. The same calculations were done with CaO single crystals, where the surface area was estimated from SEM pictures.

Finally, iceland spar runs were used, but only after subtracting the first, fast step so as to account only for the rate after the external crust has been formed, and hence after all the pores have been plugged. The comparison of these different diffusivity measurements can be seen in Figure 6.

The most obvious observation made when contemplating this Figure is the large difference in diffusivity measured with synthetic lime versus the two other samples. No explanation for this behavior has been found yet.

The second observation is that the diffusivity tends to decrease slightly with time. This could be related to a change in product layer composition with time. Most of the time, an asymptotic value could be identified. Unless otherwise indicated, that is the product layer diffusivity value that we report.

5.2.2. Product layer thickness

It is good to compare the kinetic rate with the diffusion rate so as to obtain a measure of the critical conversion where the limiting rate changes. At that point, both rates should be similar, or

$$k * C_{SO2} = D * C_{SO2}/\delta$$

or:

$$\delta = D/k$$

For the synthetic lime, this calculation gives δ=4.3 nm, which corresponds to 16 monolayers of $CaSO_4$. Because of the larger value of D obtained with iceland spar and the monocrystalline lime, the value for δ obtained there is:

δ = 553 nm, or 1317 monolayers for iceland spar

δ = 425 nm, or 1012 monolayers for monocrystalline lime

These last numbers are large, but considering the macroscopic size of the samples, they only correspond to a few percent conversion (about 8% for monocrystalline lime.)

5.2.3 Reaction order

Similar runs were made at various SO_2 concentrations. If product layer diffusion is the limiting rate, a first order in SO_2 concentration is expected. Table 1, however, show some of our results, that indicate an SO_2 order between 0.3 and 0.6.

TABLE 1
Rate at 800°C, 5% O_2 and balance He

Conc SO_2 (ppm)	init. rate (mol/s m_2)	Rate at 16% Conv (mol/s m^2)
25	$0.54*10^{-6}$	$0.28*10^{-6}$
140	$1.5 *10^{-6}$	
500	$6.4 *10^{-6}$	$1.1 *10^{-6}$
3000	$8.5 *10^{-6}$	$2.5 *10^{-6}$
8100	$8.8 *10^{-6}$	$4.6 *10^{-6}$

The order for the data reported here goes from 0.46 for the initial rate, to 0.61 at 16% conversion. Borgwardt, 1986, was the only author to investigate this issue and found an order of 0.62. It must be noticed, however, that the author did not mention at what conversion his rates were measured. He assumed a constant product layer diffusion rate and fitted his conversion measurements to this diffusivity. We noticed, as mentioned earlier, that the diffusivity changes with time. Therefore, the time, or conversion at which the measurement was made is an important piece of information.

This half order can be interpreted in two ways. Either SO_2 is not the diffusing compound, but must first undergo a reaction in which its order is one half, or the product layer created by a smaller concentration of SO_2 produces a larger diffusivity. In any case the diffusivity reported here are based on the bulk gas SO_2 concentration. In other words, Fick's law claims:

$$F = D * \nabla C = D * C/\delta$$

where F is the measured flux per unit area (proportional to the conversion rate); δ the product layer thickness and C the bulk gas SO_2 concentration. From this, we calculated D as

$$D = F * \delta/C$$

Doing so, the less than first order discussed above results in an increase in diffusivity with decreasing SO_2 concentration.

5.2.4. Activation Energy

Figure 7 shows how the diffusivity, calculated as indicated earlier, varies with temperature. Both monocrystalline lime and calcined iceland spar give reasonably similar results, except at 700 ^{o}C, where the iceland spar seems to drop to a very low rate. The activation energies, using the data shown here, are 11.6 kcal/mol for monocrystalline lime, and 18.5 kcal/mol for iceland spar. Data for the synthetic lime are also shown on this Figure. The absolute values of the diffusivities, as noticed earlier, are much lower, but the activation energy is similar (12.1 kcal/mol.)

5.3. Scanning Electron Microscopy

One way to find out whether a change in product layer composition could possibly be the reason for the observed behavior, is to observe the surface of the sulfated lime directly. Figure 8 shows the different materials that were used before reaction. After sulfation, the appearance of the samples have changed drastically, as shown in Figure 9.

The citrated (synthetic) lime, of which the granular structure was clear, has been covered with regularly shaped but randomly oriented sulfate crystals. Their size is small, but over the long run, some coarsening was noticed.

The iceland spar originally - that means, after sulfation- was composed of very fine CaO grains, but closely packed. From the pictures of sulfated iceland spar, we can easily confirm our statement that the external crust that was formed has plugged the pores. This crust is seen to consist of large, randomly oriented crystals (about 1 μm in size). It is clear, from these micrographs, that the description of the product as a homogeneous layer is bound to give results that only approximately describe the process. Micrographs of iceland spar reacted at higher temperature show larger crystals, and an orientation that is less random.

The monocrystalline lime gives the most dramatical change from all the sample studied. After having been sulfated for 16 hours, it appears porous, and has lost its original shape. When examining this sample at a lower conversion (Figure 10), the large sulfate grains appear more clearly on the surface. Their

center is a bit lower than the borders resulting in a dish-shape. This was interpreted as a predominance of grain boundary diffusion. Taken in its extreme form (diffusion occurring only at the grain boundaries, and no surface diffusion to the center), we can thus explain Figure 9a. At temperatures other than 800°C, however, the surface structure is not as dramatic, but the dish-shape is still retained.

5.4 Combination Runs

In order to determine whether a variation in product layer composition or an intermediary half order reaction is at the origin of the unexpected behavior of the diffusion rate with SO_2 concentration, combination runs were performed. When preparing a product layer by reacting our sample for a fixed time (2.5 min typically), we observed for high concentrations (>1000ppm) an order zero in SO_2. At lower concentrations, using synthetic lime, mass transfer limitations took over due to the large particle size. With iceland spar, an order 1/2 was observed (see Fig 11.)

From these observations, we can conclude that a saturation phenomenon is occurring: whatever the diffusing compound is (SO_2, S, SO_4^{--} or Ca^{++} and O^{--}), the driving force reaches a plateau when the SO_2 concentration exceeds 1000ppm. This indicates that the SO_2 dependence of the rate observed in continuous runs must be solely due to changes in composition of the product layer. At lower concentrations, the half order indicates that SO_2 is not the diffusing species as such. It probably undergoes a chemisorption that creates an activated form of sulfur, whose

concentration, at thermodynamic equilibrium, is proportional to the square root of the SO_2 concentration in the gas.

Similar experiments were done varying the temperature. The activation energy could provide a clue as to the rate limiting phenomenon. Figure 12 shows the Arrhenius plot of the reaction rate on iceland spar, after 2.5 minutes reaction with 3000ppm SO_2 at 800°C. It gives us the activation energy in the half order region (@65ppm SO_2, E_a=11.1 kcal/mol) and in the plateau region (@3000ppm SO_2, E_a=10.4 kcal/mol). The similarity in activation energy points out that the limiting rate is probably the same. This activation energy, however is very small for solid state diffusion. That is why, again, grain boundary diffusion was considered.

A last series of experiments was done, this time varying the initial reaction conditions. Since it was observed that larger grains were formed at higher temperature, we sulfated the samples to a similar conversion -same product layer thickness-, but at different temperatures, as a first sulfation step. The time for this step was calculated assuming an activation energy of 16 kcal/mol. The sample was then brought to 800°C, and sulfation resumed.

The results are shown in Table 2. As expected, the lower temperature preparations yield a faster rate at 800°C. This proves that grain size has an impact on the rate, and hence, that the activation energy measured in the continuous runs is only an apparent activation energy.

TABLE 2

Initial rate after sulfation at various temperatures to 37% conversion

Iceland Spar; 3000ppm SO_2; 5% O_2; Rate measured at 800°C

Temp. of prep. °C	time of prep. min	Conversion %	Rate 10^{-6} mol/g s
650	17.0	36.6	1.60
700	11.0	37.4	1.23
750	7.2	38.2	1.01
800	5.0	36.0	0.79
850	3.6	36.4	0.66

6. CONCLUSION AND FUTURE WORK

Two questions are focused upon during this work. At the one hand, we want to understand what the diffusing species are, or in other words, what controls the driving force. At the other hand, we want to understand the composition of the product layer, so as to find out how to model the diffusivity.

While we tried to answer these questions separately, it appears that they are linked. When the driving force, or the concentration of SO_2 gas is changed, the product layer composition, and hence the diffusivity, changes simultaneously. This complicates the interpretation of the data. That is why we designed a new series of experiments, in this work called "combination runs", in an attempt to separate these effects.

Doing so, a half order in SO_2 concentration was found at low concentrations (<1000ppm), and a zero order at high concentrations. Both of these observations indicate that SO_2 cannot be the diffusing specie. It must first be transformed to some surface specie, S^*. The surface concentration of S^* is

then limited by, at the one hand, the available surface sites (explaining the saturation phenomenon at high concentrations), and at the other hand by a chemisorption equilibrium which gives a surface concentration proportional to the square root of the SO_2 gas concentration.

The first issue that must be addressed in the coming months is the clear identification of the limiting rate. It was always assumed that product layer diffusion is rate limiting, and there is strong evidence that this is correct. However, this diffusion can occur through the lattice (extrinsic or intrinsic diffusion), through dislocations or through grain boundaries. The different aspects of the product layer for various samples, or even various temperatures, suggest that different mechanisms may be at work.

This will probably lead us to understand why the different samples yield different diffusion rates.

The next issue is the nature of the chemisorbed sulfur compound S^*. An examination of the effect of O_2 concentration might give a clue. It is also conceivable that, since this is a surface reaction, the presence of additives or of active sites will affect the reaction rate.

REFERENCES

R. Borgwardt, K. Bruce & J. Blake: "An Investigation of Product Layer Diffusivity for CaO Sulfation" Ind. Eng. Chem. Res. 26, 1993 (1987)

J. Floess, PhD Thesis, MIT, 1985

A.F. Sarofim, J.P. Longwell, G.A. Simons, D.Ham, J.C. Kramlich & G.H. Newton: "Kinetics of Sulfur and Nirtogen Reactions in Combustion Systems" Proceedings of the AR&TD Direct Utilization and Instrumentation and Diagnostics Contractors Review Meeting, 1987

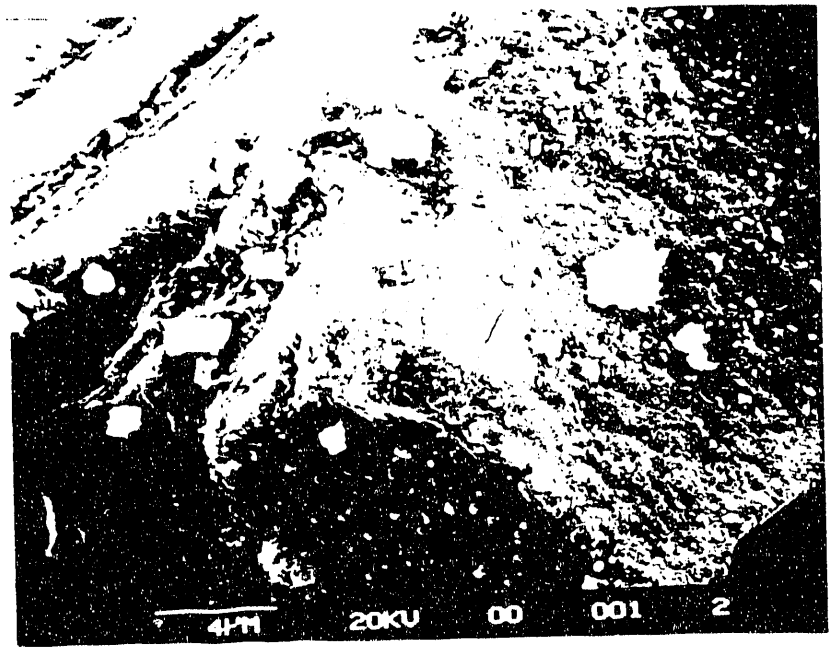

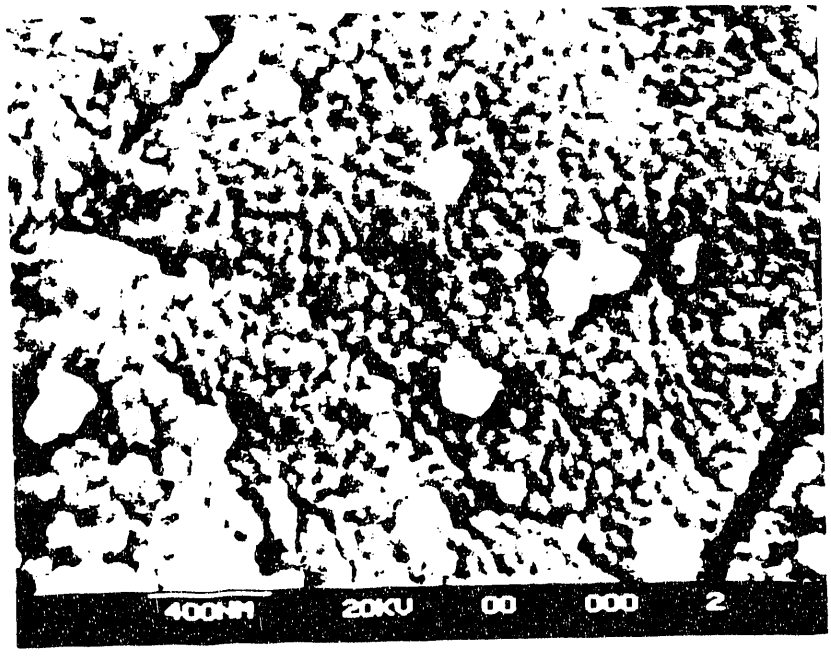

FIGURE 1: Calcined Iceland Spar

Figure 2

THE THERMOGRAVIMETRIC ANALYZER (TGA)

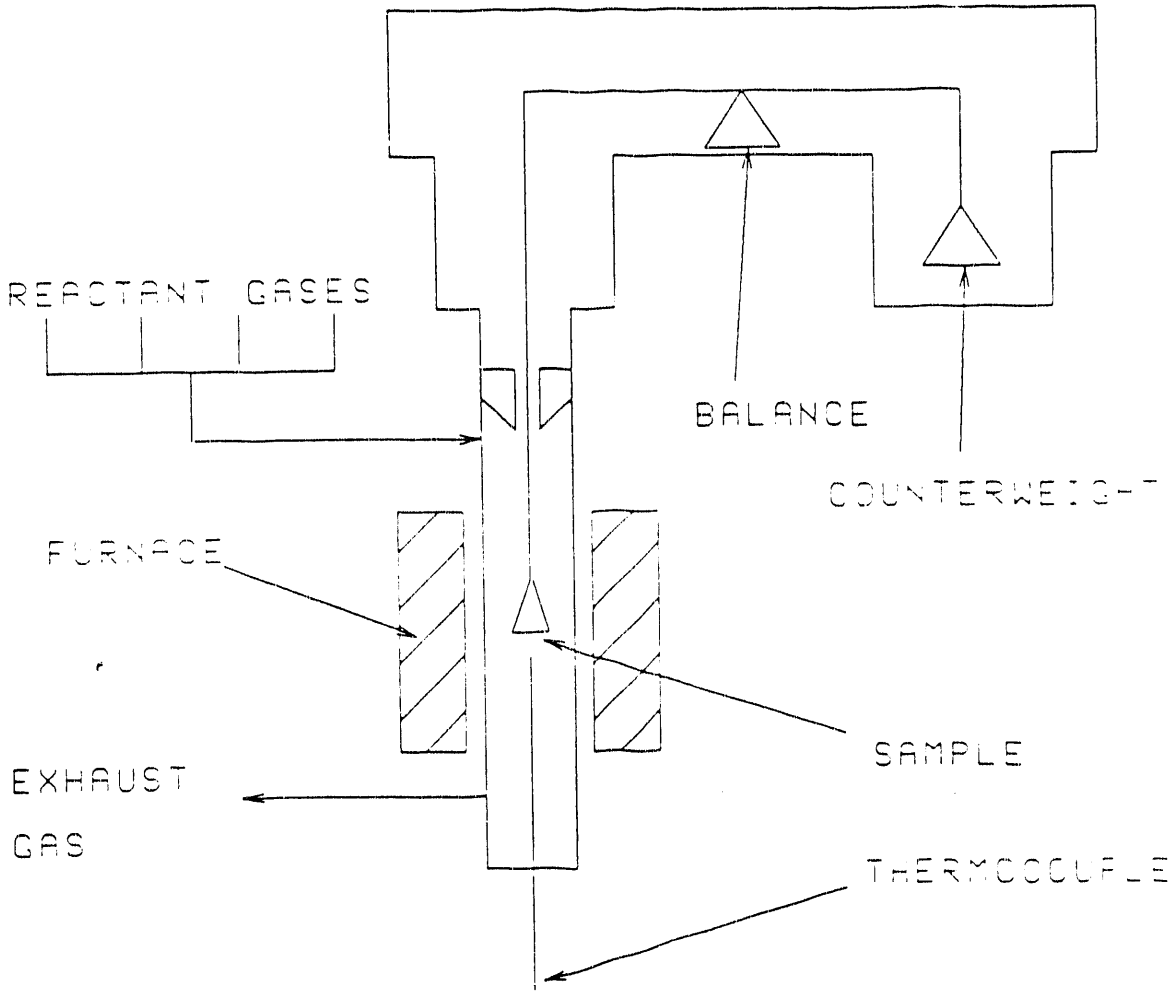

Typical Experimental Conditions:

Flow Rate: 200 SCCM

Gas Composition: 3000 ppm SO_2 ; 5% O_2 ; 95% He

Temperature: 800^{o}C

Figure 3

Product Layer Diffusivity as a function of time

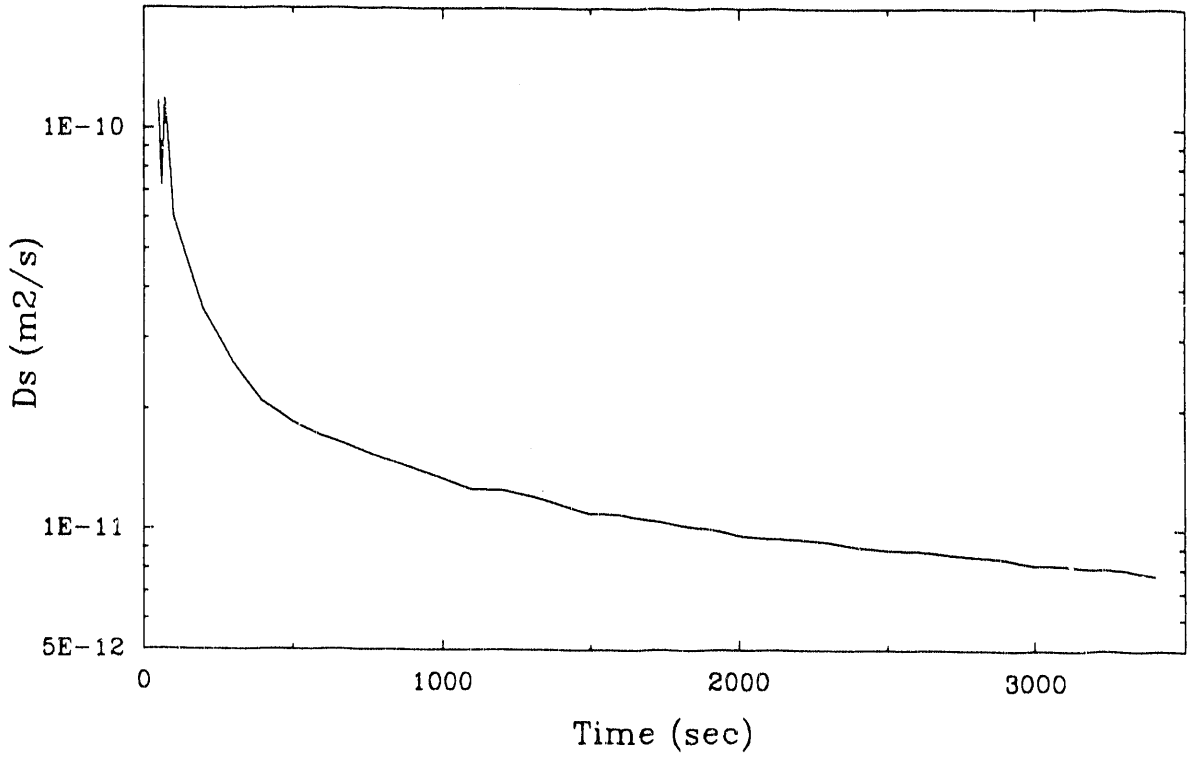

Figure 4

Combination run: example of weight and temperature profiles

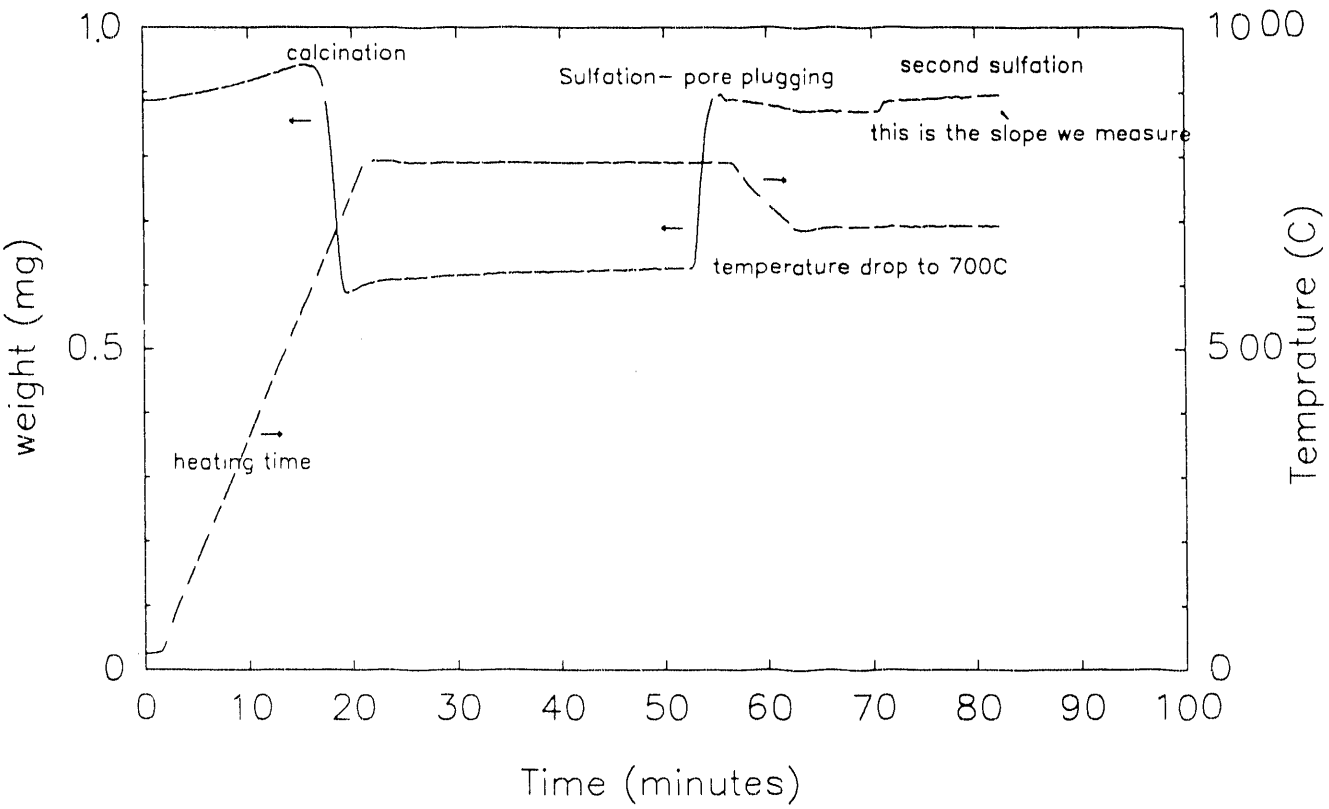

Figure 5

Arrhenius Plot for Initial Rate

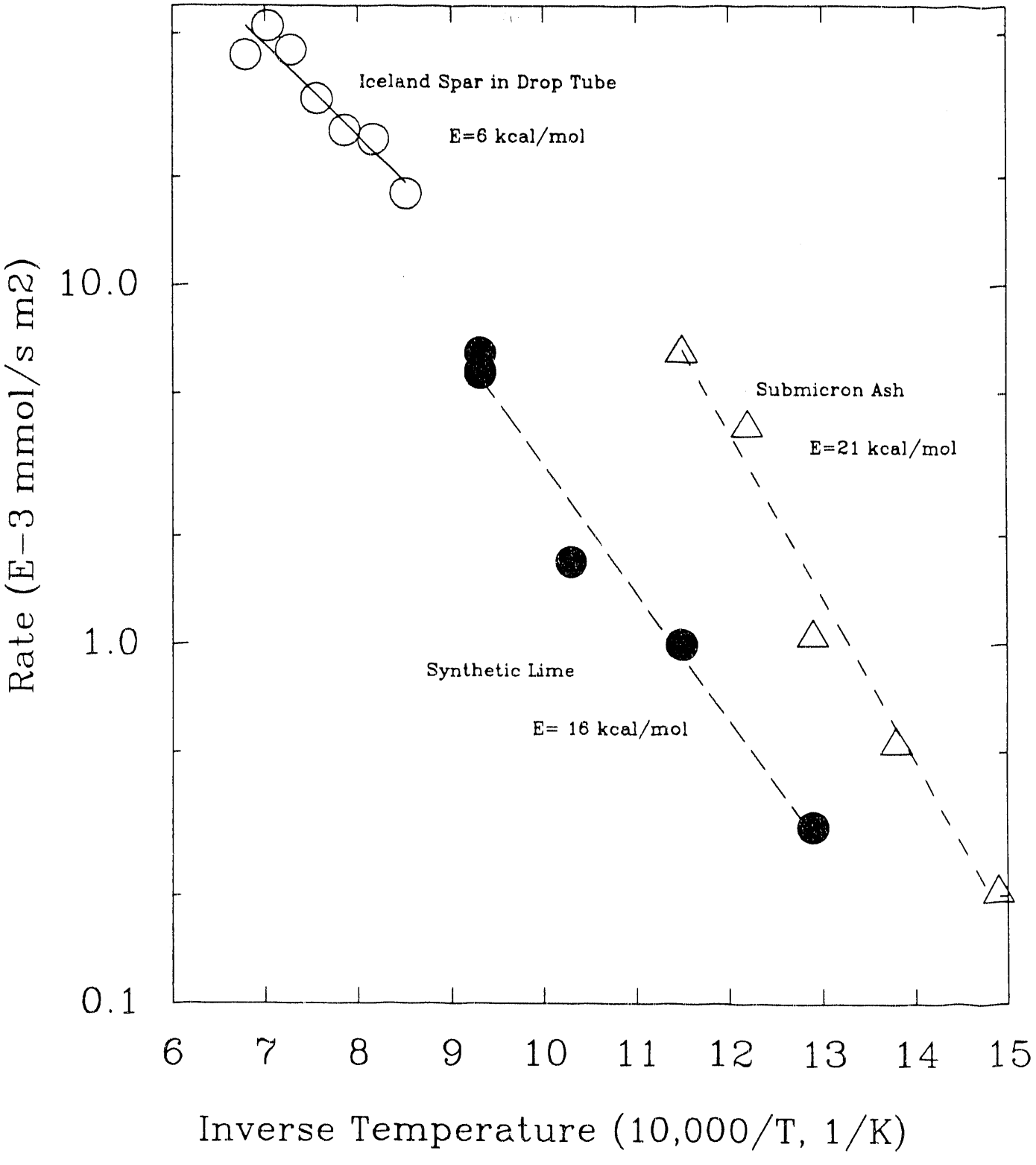

Figure 6

Comparison of the diffusivity behavior of different samples

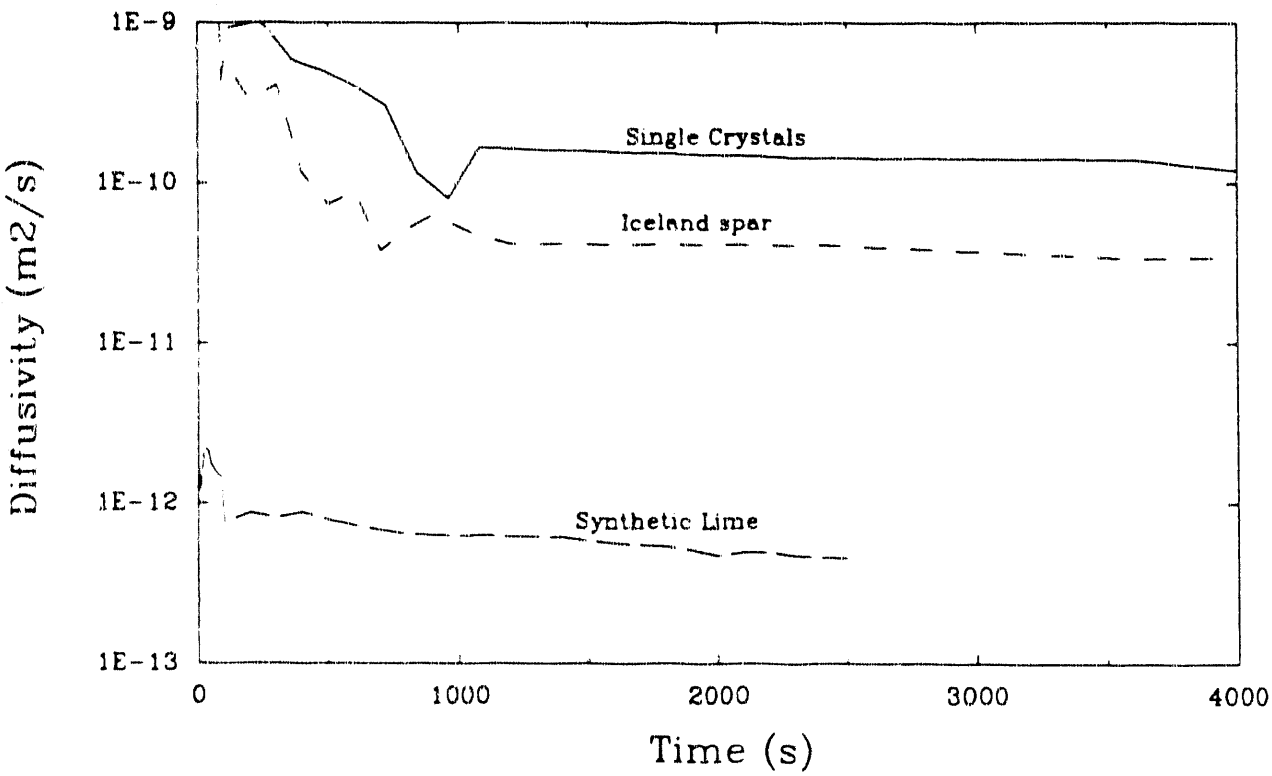

Figure 7

Temperature dependence of solid state diffusivities

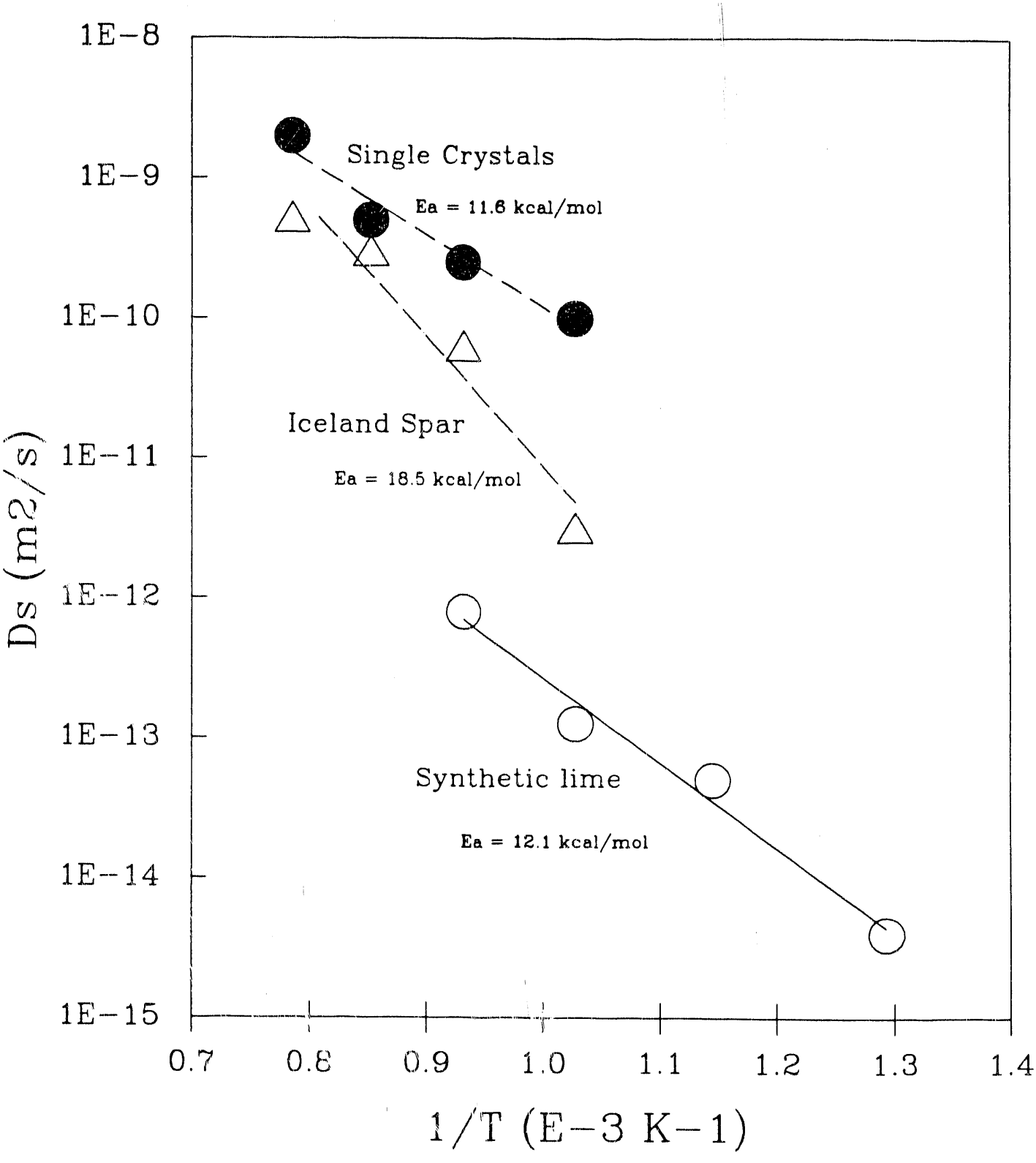

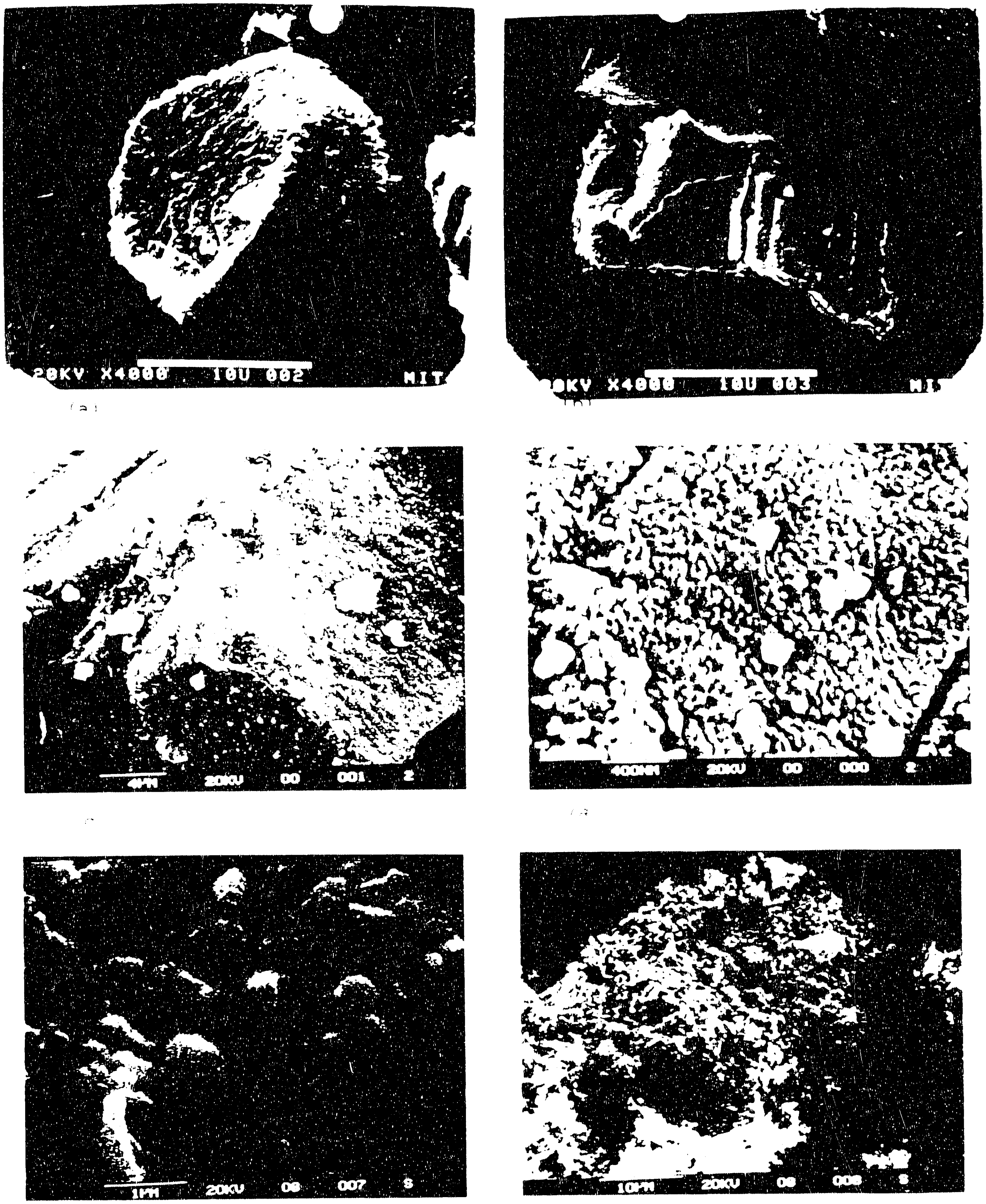

Figure 6: Micrographs of [illegible] samples used [illegible]

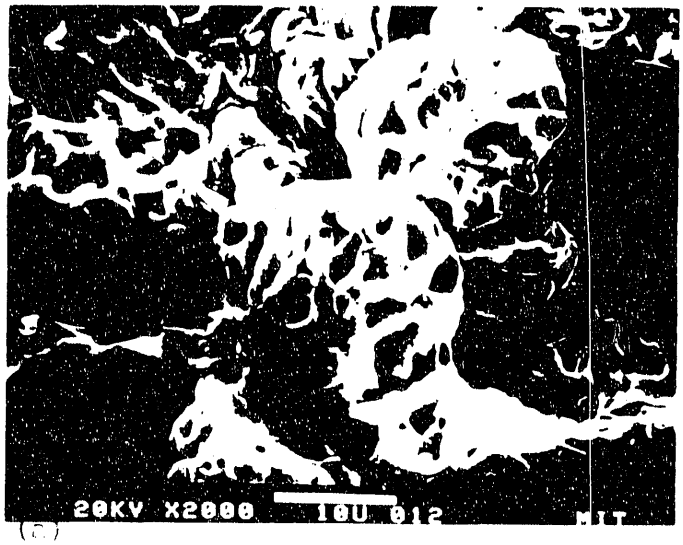

(a)

(b)

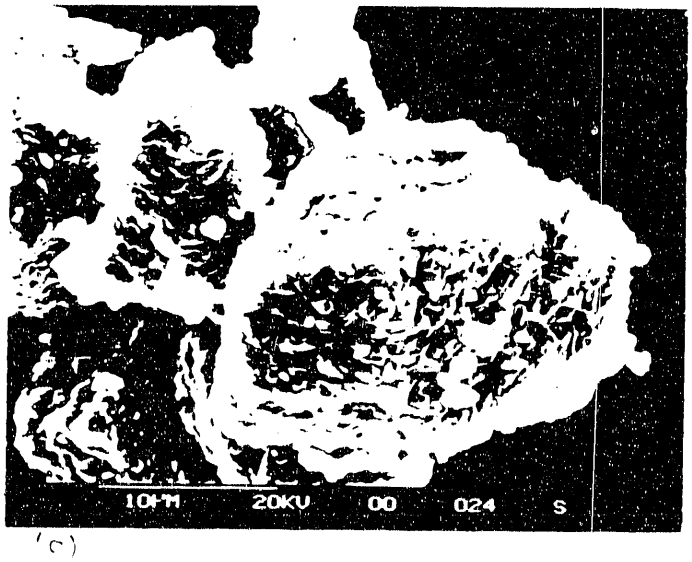

(c)

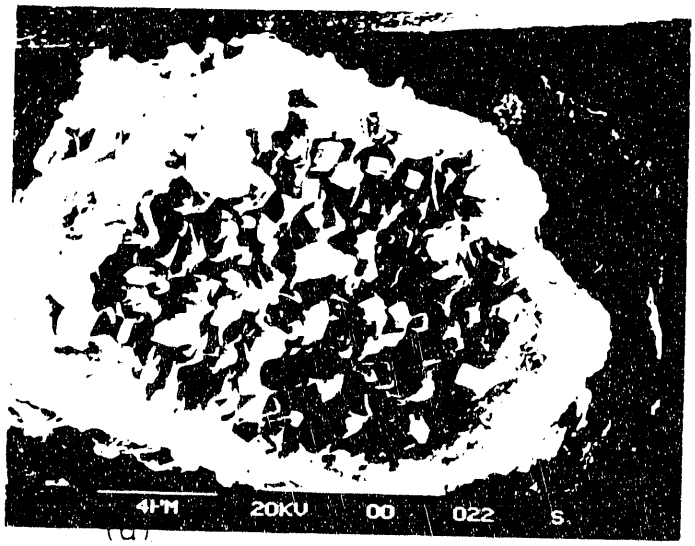

(d)

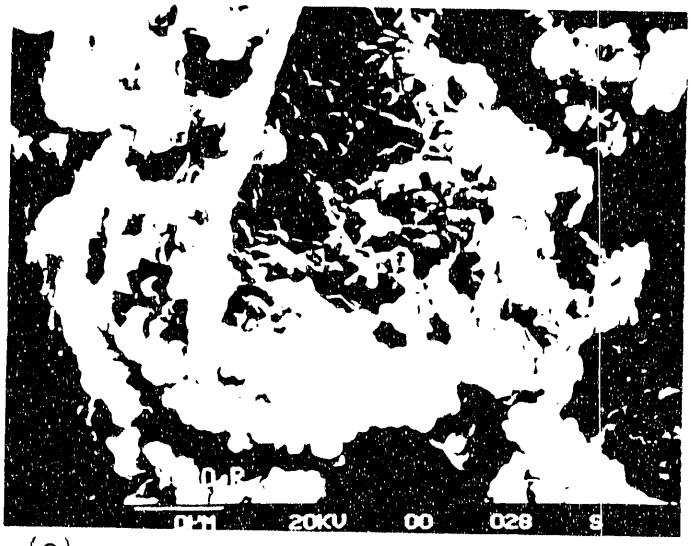

(e)

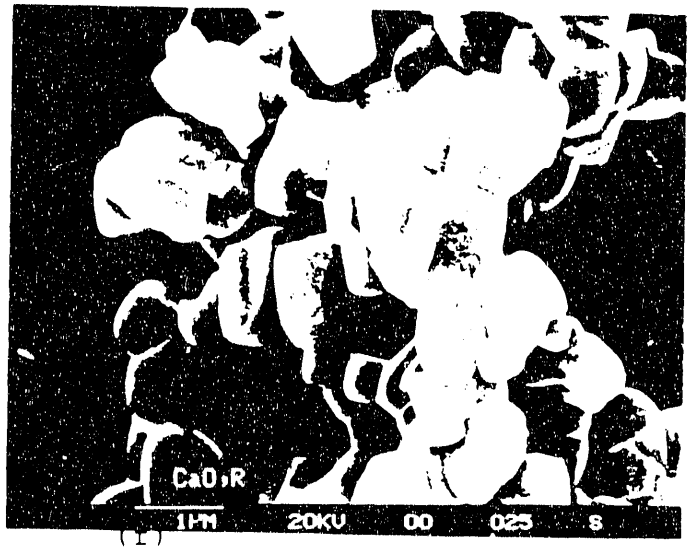

(f)

Figure 9: Microscopic aspects of sulfated CaO
(a) and (b): Single crystals; (c) and (d): iceland spar
(e) and (f): Citrated CaO

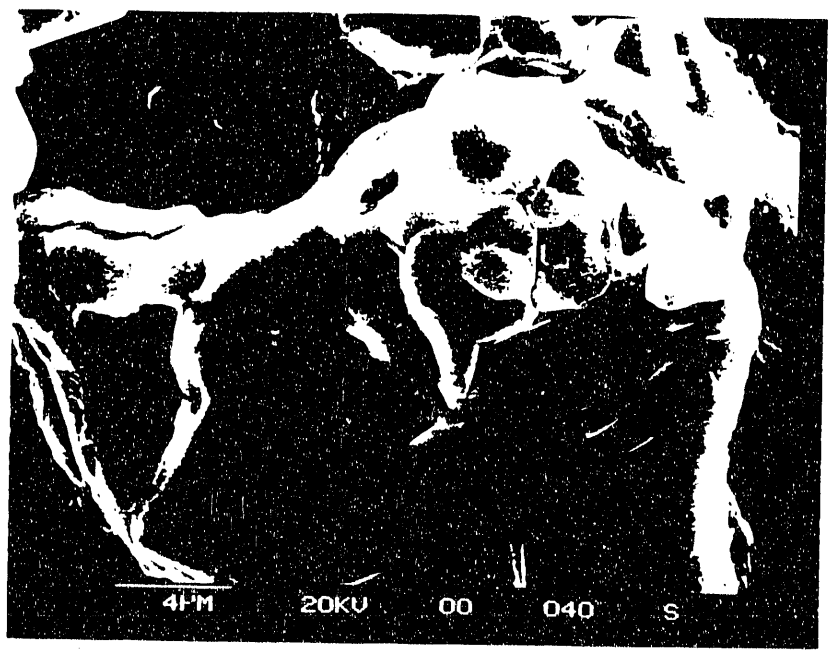

Figure 10: CaO Single crystal after 40 minutes sulfation

Figure 11

Sulfation rate of iceland spar (combination runs)

Prepared at 800C, with 5% 02 and 3000ppm S02 for 2.5 mins

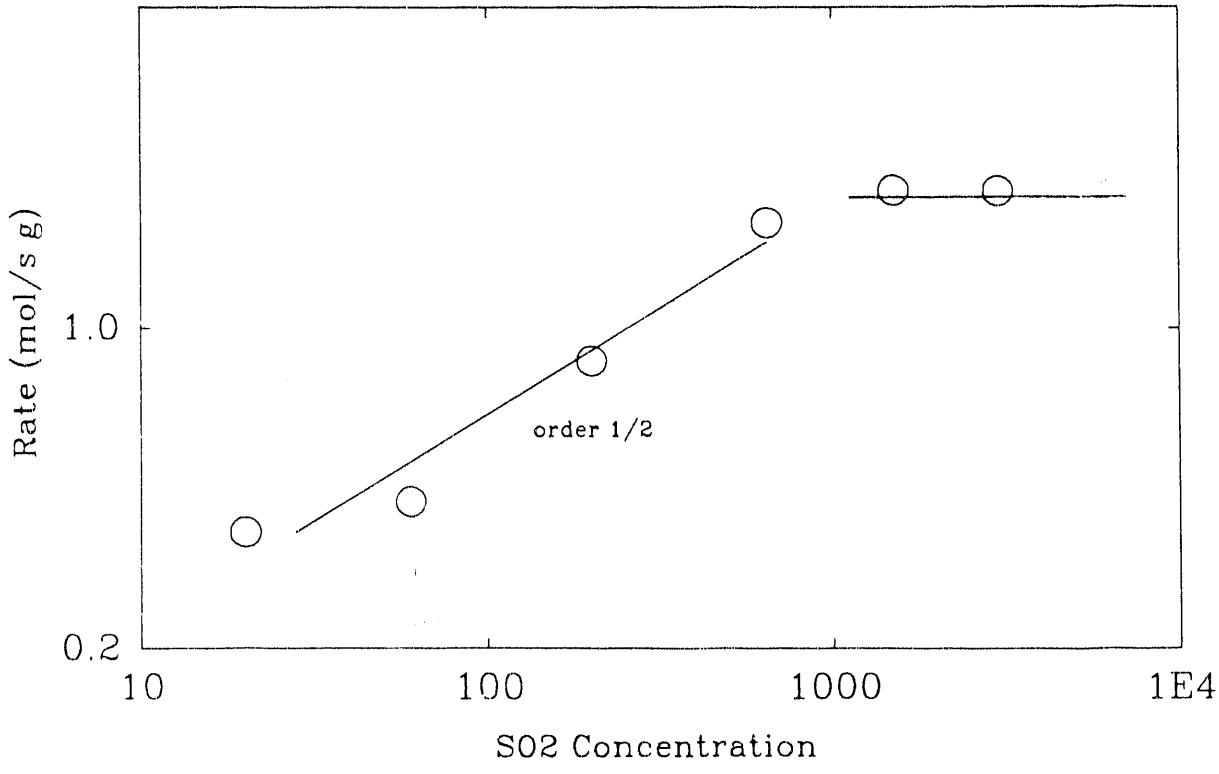

Figure 12

Temperature dependence of the diffusion rate
In the zeroth order and the half order region

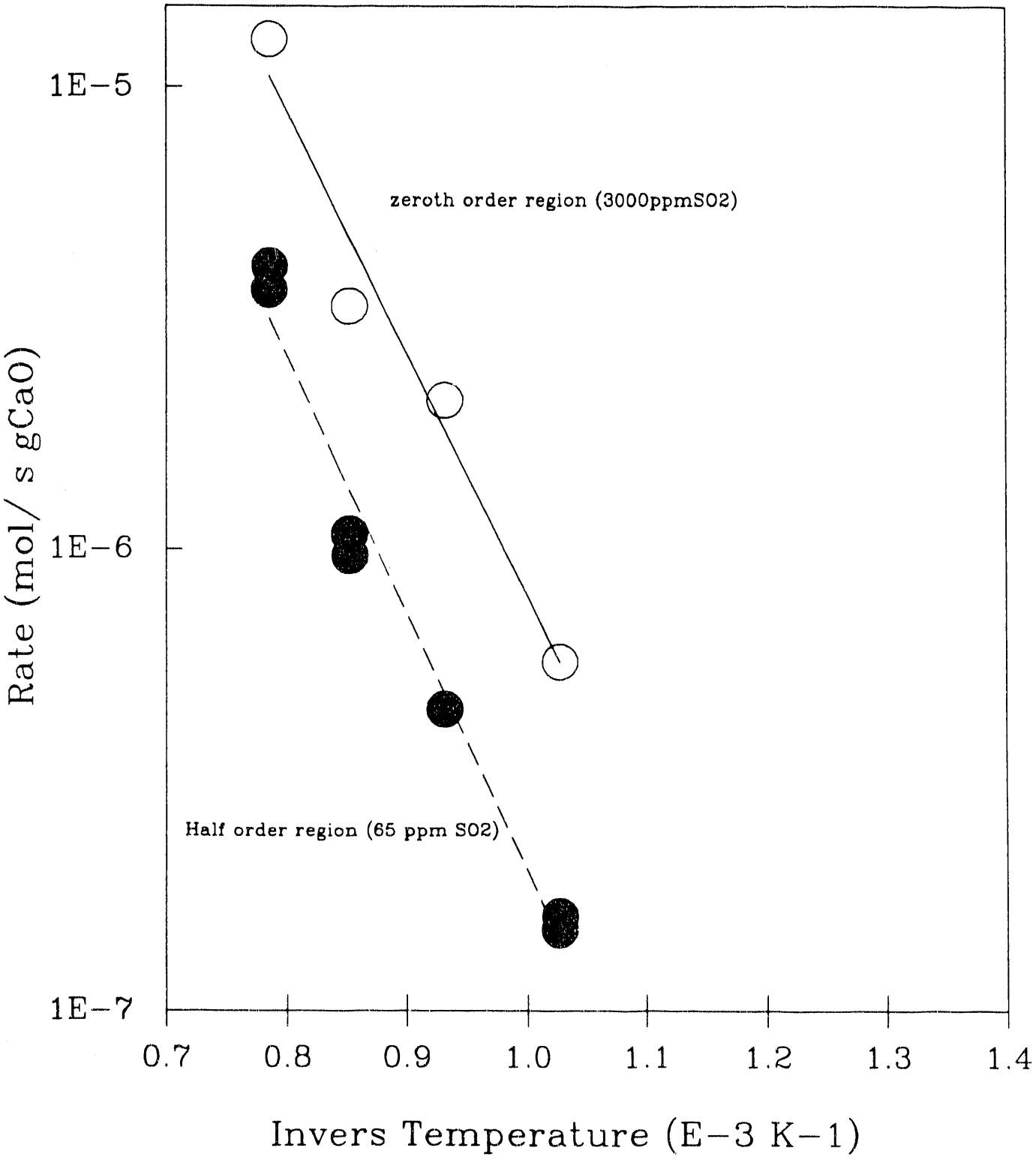

END

DATE FILMED

9/9/92